

LOW-RESOLUTION CHEST X-RAY CLASSIFICATION VIA KNOWLEDGE DISTILLATION AND MULTI-TASK LEARNING

Yasmeena Akhter, Rishabh Ranjan, Richa Singh, Mayank Vatsa

IIT Jodhpur, India

ABSTRACT

This research addresses the challenges of diagnosing chest X-rays (CXRs) at low resolutions, a common limitation in resource-constrained healthcare settings. High-resolution CXR imaging is crucial for identifying small but critical anomalies, such as nodules or opacities. However, when images are downsized for processing in Computer-Aided Diagnosis (CAD) systems, vital spatial details and receptive fields are lost, hampering diagnosis accuracy. To address this, this paper presents the Multilevel Collaborative Attention Knowledge (MLCAK) method. This approach leverages the self-attention mechanism of Vision Transformers (ViT) to transfer critical diagnostic knowledge from high-resolution images to enhance the diagnostic efficacy of low-resolution CXRs. MLCAK incorporates local pathological findings to boost model explainability, enabling more accurate global predictions in a multi-task framework tailored for low-resolution CXR analysis. Our research, utilizing the Vindr CXR dataset, shows a considerable enhancement in the ability to diagnose diseases from low-resolution images (e.g. 28×28), suggesting a critical transition from the traditional reliance on high-resolution imaging (e.g. 224×224).

Index Terms— Low Resolution, Chest X-rays, Disease Detection, CAD, Knowledge Distillation, Multitask learning

1. INTRODUCTION

Early and precise disease detection in modern healthcare is vital, with chest X-ray (CXR) imaging being a critical tool for identifying various thoracic and pulmonary diseases. Generally, high-resolution (HR) images are needed for detailed and accurate diagnoses. However, low-resolution (LR) CXRs are often used, especially in urgent scenarios or in regions with limited access to advanced imaging technology, leading to challenges in clarity and detail. The emergence of AI and deep learning in chest disease diagnosis has significantly advanced the field, with AI algorithms being adapted to address the challenges of LR images [1].

Various strategies have been proposed to improve deep-learning performance on LR images, including self-supervised pre-training, knowledge distillation (KD), and generating super-resolution images. However, each approach has limita-

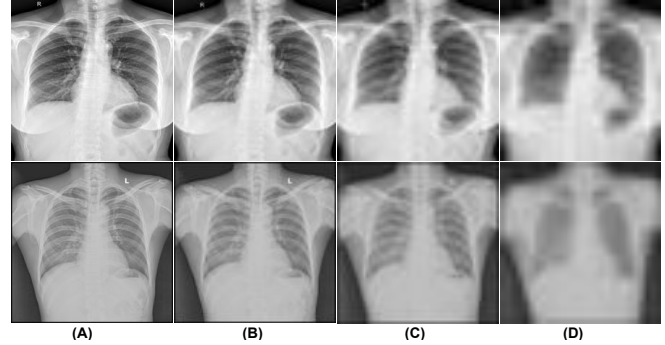


Fig. 1. Illustrating visual differences in the CXR samples. (A): HR sample of 224×224 resolution. (B)–(D): Corresponding LR samples of resolution 112×112 , 56×56 , 28×28 respectively. Downsizing leads to loss of spatial information, resulting in poor diagnostic performance.

tions, such as data scarcity for pre-training and computational inefficiency in generating super-resolution images. We investigate knowledge distillation (KD) as a means to enhance the performance of deep learning models when applied to LR images. The concept of KD, initially introduced by Hinton et al. [2], involves transferring knowledge acquired by a large teacher network to a smaller student network. KD is further classified into three types based on the nature of knowledge transfer: response-based [2, 3], features [4, 5, 6, 7], and relation-based [8, 9, 10]. Response-based KD distills ‘dark knowledge’ from the teacher network to the student network through predictions (referred to as “Soft logits”). However, it lacks the ability to convey representational information from intermediate layers and heavily relies on the final prediction layer of the teacher model. Consequently, the student lacks supervision of knowledge from the intermediate layers. On the other hand, feature-based KD necessitates an equivalent size of features in the hint and guide layers of the teacher and student models, respectively.

This research focuses on KD, as a method of transferring knowledge from the HR teacher network to the LR student network. It employs response-based and feature-based distillation, involving knowledge transfer at multiple layers. This enhances the diagnostic performance of LR CXRs. The dis-

titled knowledge includes self-attention and soft logits from Vision Transformers (ViT). The research introduces a novel framework (MLCAK) for disease diagnosis in LR CXRs using KD, marking a novel effort in this field and showing significant diagnostic improvements even with very LR inputs such as images of size 28×28 .

2. RELATED WORK

In this section, we will cover the existing works for LR and KD with respect to CXR image analysis.

Low Resolution Haque et al. [11] examined the impact of image resolution on chest X-ray detection, revealing that tasks with larger receptive fields benefit from downscaled input. Sabottke and Spieler [12] evaluated CXR performance at different resolutions, finding varying class behaviours and emphasizing the importance of identifying the class of interest. Guan et al. [13] analyzed resolution effects on pathology detection, observing diverse performances and higher resolution efficacy for certain pathologies. Li et al. [14] employed a multi-resolution ensemble for lung nodule detection in CXRs. **Knowledge Distillation** Termritthikun et al. [15] proposed KD for model compression for edge device-based CXR classification using GradCAM [16] distillation. Park et al. [17] utilized self-supervision and self-training in KD for CXR-based disease classification with noisy data. Li and Xu [18] introduced Bootstrap KD to enhance label quality and reduce noise in CXR datasets. Ho et al. [19] compared saliency mapping techniques in KD for improving CXR-based disease classification. Wang et al. [20] applied ConvNet teacher and DieT [21] as a student for COVID-19 prediction. Schaudt et al. [22] proposed PneuKnowNet, distilling knowledge from CXR annotations for pneumonia prediction. Chen et al. [23] introduced semantic similarity graph embedding for visual semantics in teacher-student KD.

In contrast to existing works on KD for model compression, we concentrate on enhancing diagnostic predictions in low-resolution data modelling by applying KD. We aim to improve multi-label classification and overall diagnostic labelling (normal or abnormal) for given CXRs.

3. PROPOSED MLCAK FRAMEWORK

We propose a multi-task KD approach that optimizes two tasks: Multi-Label Classification (*MLCT*) for identifying diseased areas in chest X-rays, and Multi-Class Classification (*MCCT*) for distinguishing between normal and abnormal classes. *MLCT* focuses on local label information, while *MCCT* captures global information. This synergistic approach enhances the model’s explainability in predicting whether a given sample is normal or abnormal, thus improving the diagnostic reliability of the network.

As shown in Fig. 2, MLCAK employs knowledge distillation to transfer knowledge from a teacher model T trained on

High-Resolution (HR) images to a student model S trained on Low-Resolution (LR) CXRs. *Vision Transformers*, ViT, [24] have demonstrated significant success in diverse classification tasks. For the model selection of T and S , we opt for the widely-used Transformer-based deep models, specifically the ViT. ViT showcases the attribute of self-attention, surpassing the state-of-the-art results previously attained by deep Convolutional models in computer vision tasks. In this study, three ViT variants, ViT_{Base} , ViT_{Small} , and ViT_{Tiny} , are chosen for both T and S . T is trained on HR CXRs with a resolution of 224×224 . We configured the LR CXRs for three settings: 112×112 , 56×56 , and 28×28 . Both T and S are pre-trained models initially trained on the ImageNet [25] dataset with a patch size of 16×16 and an input dimension of 224×224 . Subsequently, we fine-tuned these pre-trained models on the CXR dataset 4, utilizing transfer learning to enhance the generalizability of both models for the classification task.

Multi-Level Collaborative Attention Knowledge (MLCAK): Let x be the input image, X the sequence through patch embedding, and H_i the output of the i -th encoder layer. *MLCAK* is calculated as the mean of H_i for N blocks:

$$MLCAK = \frac{1}{N} \left(\sum_{i=1}^N (H_i) \right). \quad (1)$$

The idea behind transferring the *MLCAK* allows the student S trained on LR to learn from HR CXRs and focus on critical information to enable better performance on the given LR input. *MLCAK* takes two inputs simultaneously, where T takes HR and S takes its corresponding LR CXR. HR input has access to rich spatial information, and *MLCAK* aims to boost the performance of S fed with LR input. In this work, we set the value of N equal to 12 for each pair of teacher and student.

Collaborative Knowledge Distillation: Since the overall approach consists of an MTL-based setup, consisting of two tasks: *MLCT* and *MCCT*. Thus, allowing two response-based (soft logits) knowledge distillations from *HR Teacher* to *LR Student* model. Both tasks are optimized using Binary Cross Entropy (BCE) loss. *MLCT* distils soft logits as local knowledge to induce model explainability and improve overall *MCCT*. In this work, we have focused on a binary classification task with normal and abnormal class labels, termed as *global labels*, and the number of classes can be extended based on the use case. The soft logits from two tasks and the *MLCAK*, both form collaborative knowledge distillation and the distillation between the *HR* teacher and *LR* student is optimized using Mean Squared Error (MSE) loss.

$$L_{MSE} = \frac{1}{N} \sum_{i=1}^N (T_i - S_i)^2. \quad (2)$$

where T_i and S_i , represent the knowledge components of T and S for N training data samples.

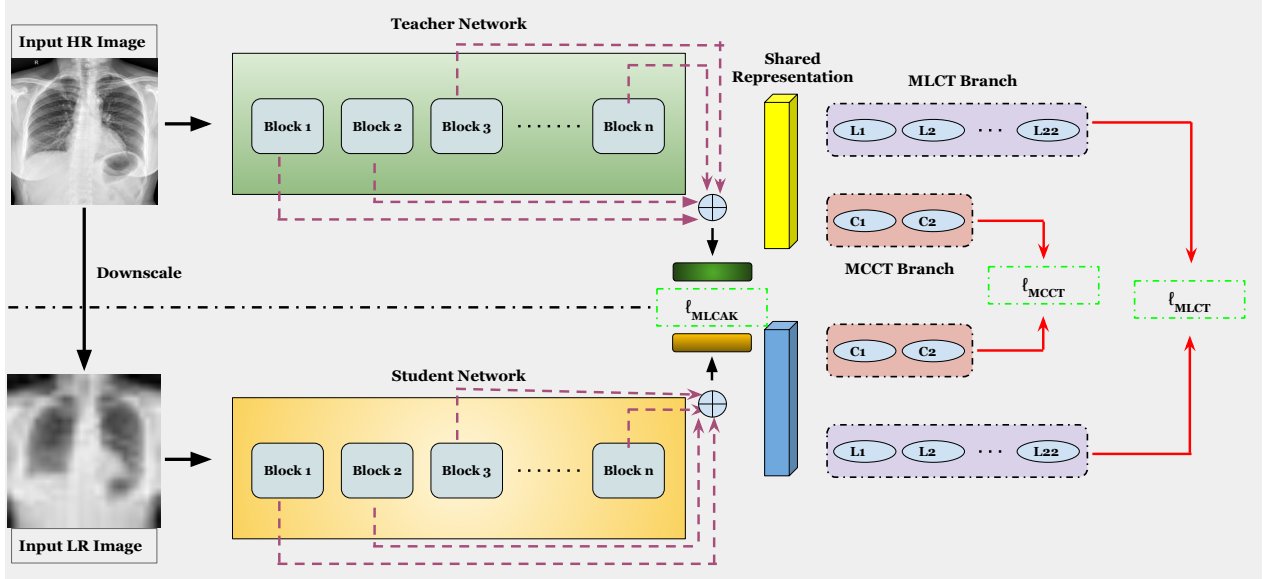


Fig. 2. Showcases the overall proposed KD approach. It takes two inputs simultaneously, where T takes HR and S takes its corresponding LR CXR and generates two outputs in the MTL setup. L_{MLCAK} , L_{MCCT} and L_{MLCT} represent the three individual losses for Collaborative Knowledge Distillation.

Joint Optimization for Student, S: The student model S is optimized by minimizing the joint loss, L_{joint} comprising of four individual losses between T and S components as given in Eq.3, where α , β , and γ are weight parameters.

$$L_{KD} = \alpha L_{mse}(MLCT) + \beta L_{mse}(MCCT) + \gamma L_{mse}(MLCAK)$$

$$L_{Classification} = L_{BCE}(MLCT) + L_{BCE}(MCCT)$$

$$L_{joint} = L_{KD} + L_{Classification} \quad (3)$$

4. EXPERIMENTAL SETUP

VinDr CXR Dataset: It consists of 18,000 posterior-to-anterior (PA) CXRs, 15,000 samples for training and 3,000 for testing. There is a total of 22 findings, which include Aortic enlargement, Atelectasis, Calcification, Cardiomegaly, Consolidation, Interstitial lung disease, Infiltration, Lung Opacity, Nodule/Mass, Other lesions, Pleural effusion, Pleural thickening, Pneumothorax Pulmonary fibrosis and No finding. We converted DICOM to PNG format and resized it to 224×224 for HR settings. We further downscaled the input to 112×112 , 56×56 and 28×28 as three LR settings. The samples of the dataset with HR and corresponding LR are shown in Fig.1.

Evaluation Metrics The effectiveness of the proposed approach is demonstrated using the Area Under the ROC Curve (AUROC) for both tasks.

Implementation Details The approach is implemented using Pytorch¹ framework. The pretrained models are downloaded

¹<https://pytorch.org/docs/stable/index.html>

Table 1. Baseline results (AUC) corresponding to different variants of ViT across different input resolutions. HR and LR refers to High Resolution and Low resolution respectively. T1 and T2 represent $MLCT$ and $MCCT$, respectively.

Model	Task	$HR_{Tr224 \times 224}$	$LR_{St112 \times 112}$	$LR_{St56 \times 56}$	$LR_{St28 \times 28}$
Tiny	T1	0.8343	0.8309	0.8057	0.7977
	T2	0.8696	0.8534	0.8505	0.8350
Small	T1	0.8563	0.8426	0.8342	0.8186
	T2	0.9010	0.8667	0.8588	0.8476
Base	T1	0.8600	0.8724	0.8260	0.7941
	T2	0.9064	0.8897	0.8795	0.8269

from <https://huggingface.co/docs/transformers/index>. We used a batch size of 64 and AdamW as an optimizer to reduce the joint loss for a total of 100 epochs. The initial learning rate is set to $5e-4$ and adjusted with a cosine annealing rate. Binary cross-entropy loss is used for both tasks and trained using NVIDIA V100-DGX GPUs.

5. RESULTS AND ANALYSIS

We conducted extensive experiments using three teacher-student model configurations to evaluate the performance of proposed $MLCAK$. Our focus is on enhancing diagnostic prediction in joint multi-label and multi-class scenarios within LR data modelling rather than compressing models. We maintained fixed model complexity for both teachers and students, employing three ViT variants: ViT_{tiny} , ViT_{small} , and

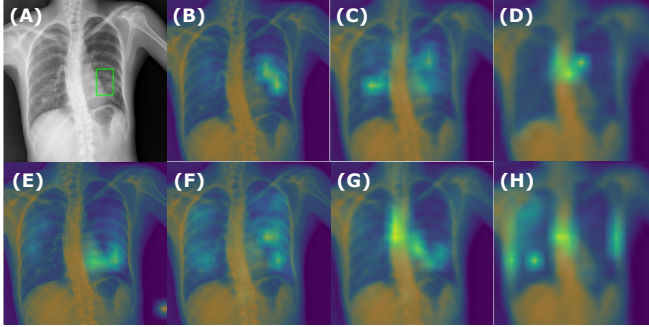


Fig. 3. Illustrates the visual difference in the attention generated by the ViT Base model. (A) Original input with finding. (B), (C), (D) are proposed *MLCAK* attention maps for the student model with resolution 112×112 , 56×56 and 28×28 respectively. (E) represent attention map from the Teacher model with 224×224 resolution and (F)-(H) baseline student model with resolution 112×112 , 56×56 , 28×28 respectively.

ViT_{base}. The proposed *MLCAK* outperforms low and high-resolution models, as evidenced by the improved AUROC for *MLCT* and *MCCT* compared to existing KD methods. Table 1 represents the results obtained without any KD scheme and are set as the baselines. We have compared the proposed KD scheme with the existing KD method, vanilla KD [2]. To emphasize the importance of the proposed knowledge transfer from *HR* teacher to *LR* student, we experimented with distilling knowledge from individual blocks of the teacher model represented as 1:1 attention transfer in Table 2. Moreover, instead of transferring the individual blocks, we used the last attention block as knowledge along with the dark knowledge of the teacher model. Notably, even at the lowest resolution (28×28), there is a significant enhancement for both tasks. We conducted experiments with changing the complexity of the teacher and student models to assess *MLCAK*'s effectiveness across different architectures. Among all, utilizing the mean, as indicated in Eq. 1, demonstrated superior performance compared to distilling the individual blocks. The results reflect task-specific performance changes during the down-sampling of CXR inputs, with *MLCT* being more affected than *MCCT*. This discrepancy arises from smaller findings in CXRs losing spatial information, requiring deeper models with higher receptive fields.

MLCAK emphasizes the significance of self-attention in ViTs, modifiable to guide student models in LR data modelling alongside traditional supervision (Fig. 3). Baseline models struggle to accurately capture diseased areas, with attention scattering (Fig. 3 (F)-(H)). An HR image with higher spatial information helps to generate well-localized attention, as shown in Fig. 3 E. As the input downscales, spatial information loss weakens attention mechanisms in localizing diseased pixels. As shown in Fig. 3, *MLCAK* leverages ViT self-attention, improving diagnostic predictions in CXRs for

Table 2. Illustrates the results (AUC) of the LR CXR-based diagnosis with the proposed *MLCAK* for MTL tasks, T1 (*MLCT*) and T2 (*MCCL*). The knowledge transfer is provided from an *HR_{T_r224x224}* in all the given cases.

Model	KD Approaches	Task	$LR_{S/112 \times 112}$	$LR_{S/56 \times 56}$	$LR_{S/28 \times 28}$
Tiny	Vanilla	T1	0.8347	0.8154	0.8068
		T2	0.8684	0.8546	0.8536
	Last Block	T1	0.8219	0.8127	0.7854
		T2	0.8654	0.8543	0.8445
	1:1 Attention Transfer (Proposed)	T1	0.8249	0.8113	0.8016
		T2	0.8640	0.8571	0.8512
MLCAK (Proposed)		T1	0.8492	0.8354	0.8202
		T2	0.8836	0.8746	0.8654
Small	Vanilla	T1	0.8562	0.8437	0.8164
		T2	0.8822	0.8727	0.8661
	Last Block	T1	0.8549	0.8437	0.8319
		T2	0.8978	0.8891	0.8703
	1:1 Attention Transfer (Proposed)	T1	0.8533	0.8437	0.8319
		T2	0.8951	0.8891	0.8703
MLCAK (Proposed)		T1	0.8717	0.8509	0.8415
		T2	0.9077	0.8904	0.8751
Base	Vanilla	T1	0.8704	0.8657	0.8238
		T2	0.8963	0.8858	0.8651
	Last Block	T1	0.8494	0.8371	0.8032
		T2	0.8892	0.8853	0.8653
	1:1 Attention Transfer (Proposed)	T1	0.8509	0.8317	0.8161
		T2	0.8878	0.8760	0.8612
MLCAK (Proposed)		T1	0.8746	0.8714	0.8387
		T2	0.8987	0.8901	0.8766

low to middle-standard infrastructure settings, thus enhancing reliability in diagnostic decisions for LR data modelling.

6. CONCLUSION AND DISCUSSION

In this research, we introduce *MLCAK*, a novel approach leveraging self-attention mechanisms within Vision Transformers, specifically designed to enhance diagnostic accuracy in scenarios with limited data availability for Chest X-rays. *MLCAK* is developed through a knowledge distillation process, where a teacher model, trained on high-resolution images, transfers its learned insights to a student model handling low-resolution CXRs. This method particularly excels in extracting and utilizing discriminating attention features in the student model, enhancing its capability to perform diagnostic tasks within a multi-task framework. A key aspect of *MLCAK* is its contribution to model explainability. It achieves this by identifying *diseased* pixels, thereby not only improving the diagnostic accuracy in low-resolution environments but also providing insights into the decision-making process of the model.

7. COMPLIANCE WITH ETHICAL STANDARDS

This research adheres to ethical standards, and all experiments conducted using the Vindr Chest X-ray dataset <https://physionet.org/content/vindr-cxr/1.0.0/>

strictly comply with the terms of use set forth by the dataset creators. The dataset utilized in this study is openly available for research purposes, and we affirm that our research does not involve any attempts at deanonymization of patients' chest X-rays. Our study prioritizes the privacy and ethical considerations associated with medical data, and we have taken measures to ensure the responsible and ethical use of the dataset in accordance with established guidelines.

8. ACKNOWLEDGEMENT

M. Vatsa is partially supported through the SwarnaJayanti Fellowship by the Government of India. This work is financially supported by the Ministry of Electronics and Information and Technology (MEITY), Government of India.

9. REFERENCES

- [1] Akhter et al., "AI-based radiodiagnosis using chest X-rays: A review," *Frontiers in Big Data*, vol. 6, pp. 1120989, 2023.
- [2] Hinton et al., "Distilling the knowledge in a neural network," *arXiv preprint arXiv:1503.02531*, 2015.
- [3] Wei et al., "Circumventing outliers of autoaugment with knowledge distillation," in *ECCV*. Springer, 2020, pp. 608–625.
- [4] Romero et al., "Fitnets: Hints for thin deep nets," *arXiv preprint arXiv:1412.6550*, 2014.
- [5] Nikos Komodakis and Sergey Zagoruyko, "Paying more attention to attention: improving the performance of convolutional neural networks via attention transfer," in *ICLR*, 2017.
- [6] Mirzadeh et al., "Improved knowledge distillation via teacher assistant," in *AAAI*, 2020, vol. 34, pp. 5191–5198.
- [7] Passban et al., "Alp-kd: Attention-based layer projection for knowledge distillation," in *AAAI*, 2021, vol. 35, pp. 13657–13665.
- [8] Yim et al., "A gift from knowledge distillation: Fast optimization, network minimization and transfer learning," in *CVPR*, 2017, pp. 4133–4141.
- [9] Seunghyun Lee and Byung Cheol Song, "Graph-based knowledge distillation by multi-head attention network," *arXiv preprint arXiv:1907.02226*, 2019.
- [10] Passalis et al., "Heterogeneous knowledge distillation using information flow modeling," in *CVPR*, 2020, pp. 2339–2348.
- [11] Haque et al., "The effect of image resolution on automated classification of chest x-rays," *medRxiv*, 2021.
- [12] Carl F Sabottke and Bradley M Spieler, "The effect of image resolution on deep learning in radiography," *Radiology. Artificial intelligence*, vol. 2, no. 1, 2020.
- [13] Guan et al., "Discriminative feature learning for thorax disease classification in chest x-ray images," *IEEE TIP*, vol. 30, pp. 2476–2487, 2021.
- [14] Xuechen Li et al., "Multi-resolution convolutional networks for chest x-ray radiograph based lung nodule detection," *Artificial intelligence in medicine*, vol. 103, pp. 101744, 2020.
- [15] Termritthikun et al., "Explainable knowledge distillation for on-device chest x-ray classification," *IEEE/ACM Transactions on Computational Biology and Bioinformatics*, 2023.
- [16] Selvaraju et al., "Grad-cam: Visual explanations from deep networks via gradient-based localization," in *ICCV*, 2017, pp. 618–626.
- [17] Park et al., "Self-evolving vision transformer for chest x-ray diagnosis through knowledge distillation," *Nature communications*, vol. 13, no. 1, pp. 3848, 2022.
- [18] Minli Li and Jian Xu, "Bootstrap knowledge distillation for chest x-ray image classification with noisy labelling," in *ICIG*. Springer, 2021, pp. 704–715.
- [19] Ho et al., "Utilizing knowledge distillation in deep learning for classification of chest x-ray abnormalities," *IEEE Access*, vol. 8, pp. 160749–160761, 2020.
- [20] Jalalifar et al., "Data-efficient training of pure vision transformers for the task of chest x-ray abnormality detection using knowledge distillation," in *EMBC*, 2022, pp. 1444–1447.
- [21] Touvron et al., "Training data-efficient image transformers & distillation through attention," in *ICML*. PMLR, 2021, pp. 10347–10357.
- [22] Schaudt et al., "Leveraging human expert image annotations to improve pneumonia differentiation through human knowledge distillation," *Scientific Reports*, vol. 13, no. 1, pp. 9203, 2023.
- [23] Chen et al., "Multi-label chest x-ray image classification via semantic similarity graph embedding," *IEEE Transactions on Circuits and Systems for Video Technology*, vol. 32, no. 4, pp. 2455–2468, 2022.
- [24] Dosovitskiy et al., "An image is worth 16x16 words: Transformers for image recognition at scale," 2021.
- [25] Deng et al., "Imagenet: A large-scale hierarchical image database," in *2009 CVPR*, 2009, pp. 248–255.